

# Numerical Solutions of the von Karman Equations for a Thin Plate

Pedro Patrício da Silva and Werner Krauth  
*CNRS-Laboratoire de Physique Statistique de l'ENS*  
*24, rue Lhomond; F-75231 Paris Cedex 05; France*  
*e-mail: patricio@physique.ens.fr; krauth@physique.ens.fr*  
(September, 1996)

In this paper, we present an algorithm for the solution of the von Karman equations of elasticity theory and related problems. Our method of successive reconditioning is able to avoid convergence problems at any ratio of the non-linear stretching and the pure bending energies. We illustrate the power of the method by numerical calculations of pinched or compressed plates subject to fixed boundaries.

PACS numbers: 02.60.Pn 02.70.Dn 46.30.Cn

The Navier-Stokes equation is not the only nonlinear partial differential equation in classical mechanics which has so far eluded a systematic analytical or numerical solution.

Notoriously difficult partial differential equations appear also in the theory of elasticity; an example is given by the von Karman equations, which describe the elastic energies governing the deformation of a thin plate [1]. The von Karman equations are simpler than the Navier-Stokes equation in that they are local, though nonlinear. A variational theorem applies, which expresses the fact that the plate searches to minimize the total elastic energy.

For a plate (described by the parametrization  $\mathbf{r}(s, t) = (x, y, z)$ ) of thickness  $h$ , the von Karman energy is given by [1]

$$\int \int \left\{ \frac{E_{el} h^3}{24(1 - \sigma^2)} \{(\Delta z)^2 - 2(1 - \sigma)[z, z]\} + \frac{h}{2} u_{ij} \sigma_{ij} \right\} ds dt \quad (1)$$

where

$$[z, z] = \frac{\partial^2 z}{\partial s^2} \frac{\partial^2 z}{\partial t^2} - \left( \frac{\partial^2 z}{\partial s \partial t} \right)^2$$

$u_{ij}$  is the strain tensor with nonlinear terms in the deformations  $u_1 = x(s, t) - s$ ,  $u_2 = y(s, t) - t$ ,  $z = z(s, t)$ :

$$u_{ij} = \frac{1}{2} \left( \frac{\partial u_i}{\partial s_j} + \frac{\partial u_j}{\partial s_i} \right) + \frac{1}{2} \frac{\partial z}{\partial s_i} \frac{\partial z}{\partial s_j}$$

$\sigma_{ij}$  is the stress tensor, linearly proportional to  $u_{ij}$ .  $E_{el}$  and  $\sigma$  are the Young modulus and the Poisson ratio, respectively.

The appropriate framework for a precise numerical solution of this elastical problem is the finite element method [2], in which the plate (described by intrinsic variables  $s$  and  $t$ ) is cut up into triangles, the corners of which come to lie at specified “nodes”. Inside each triangle, any of the three functions is interpolated by a high-order polynomial, such that it is continuously differentiable as one passes from one triangle to the next one. This ensures a well-defined energy. Classic work on the finite element method has established the existence of a “magic” polynomial of order 5:

$$x(s, t) = a_1 + a_2 s + a_3 t + a_4 s t + \dots + a_{21} t^5 \quad (2)$$

(and similarly for  $y$  and  $z$ ). The 21 parameters in eq. (2) are fixed by prescribing at the three corners the function value  $x$ , the first and second derivatives  $\partial x / \partial s$ ,  $\partial x / \partial t$ ,  $\partial^2 x / \partial s^2$ ,  $\partial^2 x / \partial s \partial t$ ,  $\partial^2 x / \partial t^2$  as well as the normal derivatives  $\partial x / \partial n$  on the midpoints of the triangle’s sides. We denote these variables of different origin by a symbol  $\xi = (\xi_1, \dots, \xi_N)$ , with  $N$  the total number of variables. The polynomial eq. (2) possesses an important symmetry property with respect to spatial rotations [2]. It uses all the 21 polynomial parameters to satisfy, in an optimal choice, the continuity of the first derivatives across the sides of the triangle. Notice that all the second derivatives of the functions are imposed at the nodes. By construction, the functions  $x(s, t)$  *etc.*, are thus twice continuously differentiable at these points.

Given the nodes, and the variables  $\xi$ , it is straightforward to compute the interpolating polynomials (in the simplest fashion by inverting a  $21 \times 21$  matrix), and to compute the *local* energy  $E(s(\xi), t(\xi))$  as well as the *total* energy  $\mathcal{E}(\xi) = \int E(s(\xi), t(\xi)) ds dt$  exactly [3].

As explained before, the finite element functions are valid variational test functions. It is therefore appropriate to search for the set of variables  $\xi$  minimizing the total energy. This multidimensional minimization problem (solve for  $\min_{\xi} \mathcal{E}(\xi)$ ) is at the heart of our present concern, and our main result will consist in an algorithm which, for the first time, makes possible a direct attack at the von Karman equations in the presence of strong deformations, and at any value of the thickness [4]. Any naive attempt to solve it is doomed to fail because of the large number of variables at hand. In addition, we have to solve the variational problem to great precision (essentially achieve  $|\nabla \mathcal{E}| = 0$ ), since we are not really interested in the numerical value of the total energy, but in the geometrical aspects of the solution, which are much slower to converge than  $\mathcal{E}$ .

A few algorithms are specifically geared at the solution of large minimization problems (for continuously differentiable functions). They all attempt a local fit of the function by a parabola

$$\mathcal{E}(\xi) \sim c + b \xi + \frac{1}{2} \xi H \xi \quad (3)$$

where  $H$  is the Hessian matrix of second derivatives. Based on the knowledge of the function and of its numerical gradient  $b$ , strategies differ on how to economize on the computation of  $H$  [5].

We have initially been extremely frustrated with the performance of these algorithms for large  $N$ , especially in the strongly nonlinear regime of small  $h$ . We illustrate the difficulties on a test example with  $N = 272$ , a compressed half cylinder (*cf* fig. 2) of thickness  $h = 0.01$ , which will be further discussed later on. The upper curve in fig. 1 shows the total energy  $\mathcal{E}$  as a function of the iteration number, using one of the standard algorithms. For the given boundary condition, the simulation has proceeded for a few weeks on our work station without achieving reasonable convergence. In particular, the iteration never exhibits the quadratic convergence rate, which is the hallmark of the fast minimization algorithms, and which allows in principle the solution of problems with hundreds or thousands of variables [5].

Before exposing our solution for the present nonlinear case (*i. e.* when  $H$  depends on  $\xi$ ), we shortly discuss the corresponding *linear* problem, in which the function  $H$  is independent of  $\xi$ . The behavior of iterative minimization routines, such as the Hestenes-Stiefel conjugate gradient method, has been discussed in the literature, (*cf* [6] for a very clear discussion). The result is that the minimization algorithm performs well if the matrix  $H$  is well conditioned or is close to the unit matrix. Preconditioning algorithms have been devised, which transform the matrix  $H$  into a similar matrix, close to the identity [6].

The fact that the nonlinear minimization program in fig. 1 initially works very badly can thus only mean one of two things: we either never enter the quadratic region, where the energy  $E(\xi)$  can be approximated by eq. (3), or we have to do with badly conditioned matrices  $H(\xi)$ . It is an explicit computation of  $H$  (which is not normally undertaken), that has convinced us on several examples that the approximation eq. (3) becomes acceptable quite early in the simulation (it is to test this hypothesis that the very long initial runs were undertaken). However, the matrix  $H$  becomes very often extremely ill-conditioned especially if  $h$  is small. In the simulation followed in fig. 1, the eigenvalues of  $H$  span 6 orders of magnitude at the point a) (specified by variables  $\xi_a$ ).

This has convinced us that a *reconditioning* of the matrix is necessary. We have used the simplest reconditioning possible: every so often, say, at point a), we explicitly compute  $H$  ( $= H(\xi_a)$ ) and its eigenvalues  $\alpha_i$  and eigenvectors  $\eta_i$ . We then choose *new* variables  $\tilde{\xi} = \eta_i / \sqrt{\alpha_i}$ . At point a), the matrix  $H$  thus ideally starts out as the unit matrix, and it then gets modified as we move away from  $\xi_a$  [7].

The expenditure of computing the matrix  $H(\xi_a)$  and of reworking the complete calculation in terms of  $\tilde{\xi}$  may seem enormous. However, it is immediately rewarded by a strong decrease in the energy, and a concomitant fast motion in the variable space. This can be seen on the middle curve in fig. 1 starting at point a). As we move away from  $\xi_a$ , the condition of  $H$  ( $\equiv H(\xi)$ ) necessarily deteriorates again. In the example of fig. 1, starting from a well-conditioned matrix at point a), we reach at point b) an eigenvalue spectrum which again spans 5 orders of magnitude. In fact, most eigenvalues are of order 1, but a few very small eigenvalues corrupt the condition of the matrix.

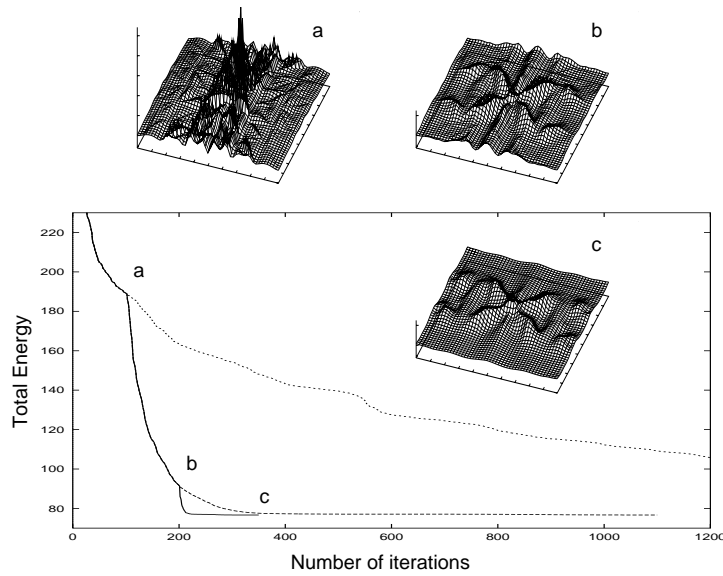


FIG. 1. Evolution of the minimization in a test case (same problem as in fig. 2,  $h = 0.01$ , 16 nodes,  $N = 272$  variables). Upper curve: total energy  $\mathcal{E}$  vs iteration using a standard conjugate gradient algorithm. Reconditioning at a) and b) leads to the lower two curves. The insets show the local energy  $E(s, t)$  at a), b) and c). The final solution is given in fig. 2.

If we continued our calculation, we would stay on the middle curve indicated in fig. 1, and undergo a gradual deterioration of the convergence. If, on the other hand, we recondition the matrix a second time, at point b), we immediately approach the solution of the problem (and witness a quadratic convergence rate (*cf* [5]), which means that we double the number of significant places of the solution *per* iteration). A zero gradient of  $\mathcal{E}$  (to machine precision) is reachable without problems.

The final approach of the convergence is usually achieved after a few reconditionings, the precise number of which depends on the physical nature of the problem. A good criterion is to try reconditioning if  $\mathcal{E}$  no longer decreases even though  $|\nabla \mathcal{E}|$  is not yet approaching 0 (which would indicate convergence). It is thus evident that reconditioning is useless in the initial stage of the minimization, in which even the standard algorithms decrease the energy

quite well. In fig. 1, we also show the local energy distribution, at points a), b) and c).

The physical problem discussed so far consists in an elastic plate, whose zero-energy configuration is the unit square. We impose a cylindrical contour on two opposing sides. In addition, the plate is compressed along these two sides, as indicated in fig. 2. In our numerical work, we have to be concerned with the existence of local minima. In order to avoid the problem, we solve the minimization problem repeatedly for increasing values of the compression. For example, in the upper part of fig. 2, we first impose the cylindrical shape, and then compute minima of the von Karman energy for increasing values of the lateral compression. For all the values of the plate thickness  $h = 0.1, \dots, 0.001$  and of the compression, we have observed no numerical problems other than a gradual increase in the number of reconditionings required as  $h$  decreases.

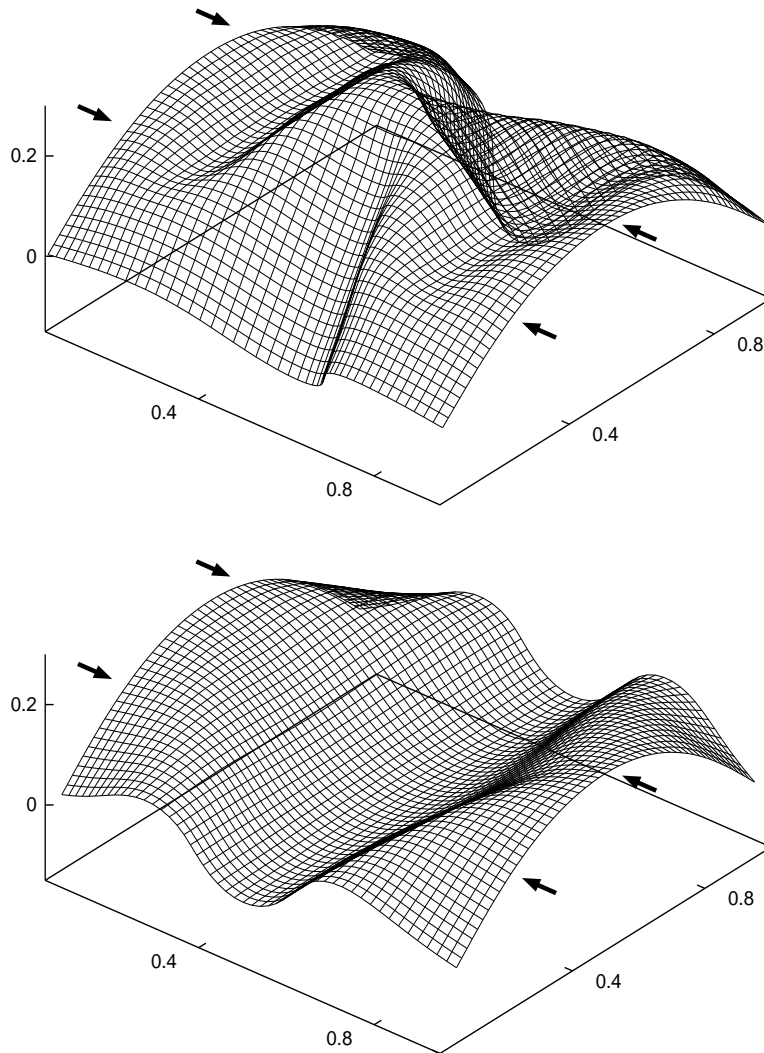


FIG. 2. Minimum energy solution for an elastic plate which was first bent, and then compressed (upper) and first compressed and then bent (lower).

In the lower part of the fig. 2, we have followed a different procedure, by first compressing the flat plate, and then gradually imposing the cylindrical outer shape, in such a way that

the final constraints are exactly equivalent in the two parts of the figure. In both cases, we have undertaken extensive tests which have convinced us that precise numerical solutions are obtained with of the order of 16 independent nodes, and a few hundred independent variables [8].

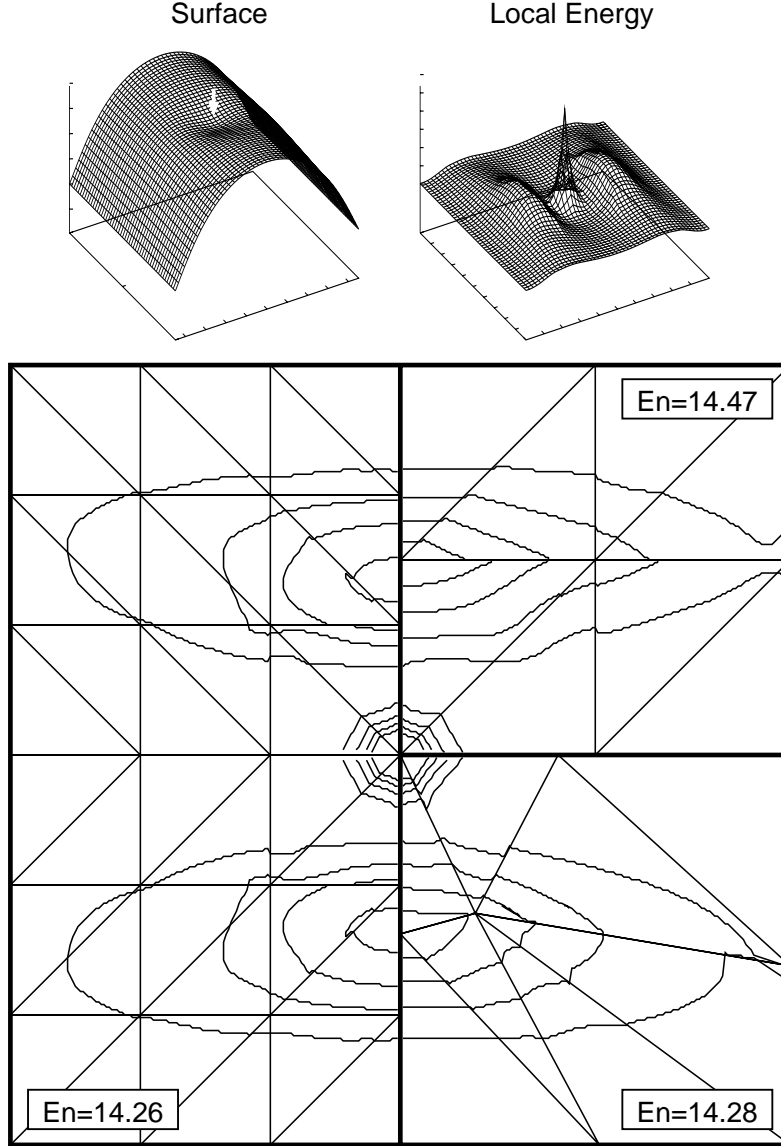


FIG. 3. Adaptive solution for the case of the pinched half-cylinder. The main figure presents contour plots of  $E(s, t)$  and the triangulation.

Left *two* quadrants: Nonadaptive calculation with  $N = 271$  variables, 16 nodes.

Right upper quadrant: Nonadaptive,  $N = 126$ , 9 nodes

Right lower quadrant: Adaptive,  $N = 126$ , 9 nodes.

The adaptive calculation with 9 nodes gives essentially the same variational energy as the non-adaptive calculation with 16 nodes. Iterative minimization was used, as described in the text.

Up to now, we have discussed the minimization problem only at fixed choice of the nodes. The most obvious way of increasing the precision of a calculation consists in adding new

ones, *e.g.* by subdividing existing triangles. This strategy has been explored in the literature [9], but soon encounters its limits as the number of variables increases very rapidly with the number of independent nodes. However, the node positions may be included in the variational problem. Let us denote the node variables by a symbol,  $\eta$ . A sharper variational function can be obtained not only by increasing the dimension of  $\eta$ , but by solving the extended minimization problem

$$\min_{\eta, \xi} \mathcal{E}(\xi(\eta)) \quad (4)$$

Just as the Gaussian integration (in which the function to be integrated is evaluated at optimal positions), we can expect substantial gains in the quality of the variational functions. To show the usefulness of the approach, we present in fig. 3 the results of three separate numerical calculations on the problem of the half-cylinder which is pinched in the middle (we begin by compressing the elastic plate into a half cylinder, and then impose a fixed position for the center of the plate, *cf.* the upper left inset in fig. 3). On the left, we show a contour plot of the energy density, and the position of the nodes for a (non-adaptive) numerical calculation with  $N = 271$  variables, and 16 nodes. On the right upper side, we show the corresponding results for a non-adaptive calculation with  $N = 126$  variables, 9 nodes, and on the right lower side an *adaptive* calculation, with the same number of nodes. There are two important features of the adaptive solution: the global energy  $E$  is of the same quality as the much more expensive, non-adaptive solution with 16 nodes. Notice that the energy density resembles much more the one of the larger calculation, and that the nodes wander into regions of large local energy.

In order to simplify the computation, we have, in fact not performed a full synchronous minimization over  $\eta$  and  $\xi$ , which seems unnecessary. In fact, it clearly appears that among the variables  $\xi$ , those which concern the function values, and the first derivatives converge much faster than the second derivatives (since the test functions are only once continuously differentiable). It is thus natural to suppose that the change of the node positions will have the largest influence on second derivatives. The minimization was done in an iterative form, in which the usual minimization ( $\min_{\xi} \mathcal{E}(\xi)$  at fixed  $\eta$ ) is supposed to yield reasonable values for the functions  $x, y, z$ , and the *first* derivatives. At fixed function values and first derivatives, we then search for optimal values of  $\eta$  and of the second derivatives, after which we again solve the usual problem, at the new  $\eta$ . This completely rigorous procedure (every function encountered is a true test function of the von Karman energy) is then iterated several times. It quickly finds better nodes, which especially show smoother variations of the second derivatives of  $x, y, z$  across the triangle boundaries.

In conclusion, we have discussed in this paper a very efficient method to solve numerically the von Karman equations. In the examples studied, our approach of successive reconditioning takes away all the convergence difficulties (in the different regimes of nonlinearity, *i. e. h*). Further work will have to show whether the reconditioning can be obtained at 'reduced cost', without computing the full numerical Hessian. We also discussed the idea of optimizing with respect to the node variables. This adaptive choice of nodes was shown to be very useful. In the example, the nodes (and the sides of the triangle) migrate towards regions of very large local energy. We think it ultimately possible to take into account non-elastic terms in the von Karman equations, and thus produce a true numerical calculation of "crumpled paper" [10]. It should be evident that the method may be of general usefulness

for non-linear minimization problems in high dimension.

Acknowledgment: We acknowledge helpful discussions with M. Ben Amar, who also got us interested in the present subject.

---

- [1] L. D. Landau and E. M. Lifshitz, *Theory of Elasticity - Course of Theoretical Physics Vol. 7*, Pergamon Press (1954)
- [2] H. R. Schwarz, *Finite Element Methods*, Academic Press (1988)
- [3] The integrals, which are all polynomials in  $s$  and  $t$ , can be computed exactly by Gaussian integration.
- [4] Most of the work has dealt with the theory of plates in the limit of small linear deformations. For large deformations, a spring model has been used within a boundary layer analysis (A. E. Lobkovsky University of Chicago preprint (1996)). Cf also T. Hughes *et al*, Eds, *Finite Element Methods for Plate and Shell Structures* Pineridge Press International, Swansea, U.K. (1986)) and M. Bernadou *Méthodes d'Eléments finis pour les Problèmes de Coques minces*, Masson (1994) who discuss several finite element *approximations* of the nonlinear problem for plate and shell theories.
- [5] W. H. Press S. A. Teukolsky, W. T. Vetterling, B. P. Flannery, *Numerical Recipes*, 2nd edition, Cambridge University Press (1992).
- [6] G. H. Golub and C. F. van Loan, *Matrix Computations* Johns Hopkins University Press (1989), chap. 10.3.
- [7] Due to numerical problems in determining  $H$  and its eigensystem for the very bad conditioning encountered, the new Hessian  $\tilde{H}$  is usually not very close to the unity matrix. The reconditioning can be iterated at the same point. The expense of doing this has to be weighted against the fact that  $H$ , of course, depends on  $\xi$ .
- [8] In both cases, we impose the symmetries  $x \rightarrow -x$ ,  $y \rightarrow -y$  of the solution.
- [9] I. Babuska, *Modeling, Mesh Generation, and Adaptive Numerical Methods for Partial Differential Equations* Springer-Verlag (1995).
- [10] M. Ben Amar and Y. Pomeau, Proc. Roy. Soc. (to appear)